



Theory of multiphoton photoemission disclosing excited states in conduction band of individual TiO_2 nanoparticles

Bochao Li(李博超), Hao Li(李浩), Chang Yang(杨畅), Boyu Ji(季博宇), Jingquan Lin(林景全), and Toshihisa Tomie(富江敏尚)

Citation: Chin. Phys. B, 2021, 30 (11): 114214. DOI: 10.1088/1674-1056/ac1b8d

Journal homepage: <http://cpb.iphy.ac.cn>; <http://iopscience.iop.org/cpb>

What follows is a list of articles you may be interested in

Selective synthesis of three-dimensional $\text{ZnO@Ag/SiO}_2\text{@Ag}$ nanorod arrays as surface-enhanced Raman scattering substrates with tunable interior dielectric layer

Jia-Jia Mu(牟佳佳), Chang-Yi He(何畅意), Wei-Jie Sun(孙伟杰), Yue Guan(管越)

Chin. Phys. B, 2019, 28 (12): 124204. DOI: 10.1088/1674-1056/ab4d45

Zinc-oxide nanoparticle-based saturable absorber deposited by simple evaporation technique for Q-switched fiber laser

Syarifah Aloyah Syed Husin, Farah Diana Muhammad, Che Azuranim Che Abdullah, Siti Huzaimah Ribut, Mohd Zamani Zulkifli, Mohd Adzir Mahdi

Chin. Phys. B, 2019, 28 (8): 084207. DOI: 10.1088/1674-1056/28/8/084207

Improved dielectric and electro-optical parameters of nematic liquid crystal doped with magnetic nanoparticles

Geeta Yadav, Govind Pathak, Kaushlendra Agrahari, Mahendra Kumar, Mohd Sajid Khan, V S Chandel, Rajiv Manohar

Chin. Phys. B, 2019, 28 (3): 034209. DOI: 10.1088/1674-1056/28/3/034209

Numerical study of optical trapping properties of nanoparticle on metallic film with periodic structure

Cheng-Xian Ge(葛城显), Zhen-Sen Wu(吴振森), Jing Bai(白靖), Lei Gong(巩蕾)

Chin. Phys. B, 2019, 28 (2): 024203. DOI: 10.1088/1674-1056/28/2/024203

Optical properties of a three-dimensional chiral metamaterial

Juan-Juan Guo(郭娟娟), Mao-Sheng Wang(汪茂胜), Wan-Xia Huang(黄万霞)

Chin. Phys. B, 2017, 26 (12): 124211. DOI: 10.1088/1674-1056/26/12/124211

Theory of multiphoton photoemission disclosing excited states in conduction band of individual TiO₂ nanoparticles*

Bochao Li(李博超), Hao Li(李浩), Chang Yang(杨畅), Boyu Ji(季博宇),
Jingquan Lin(林景全)[†], and Toshihisa Tomie(富江敏尚)[‡]

School of Science, Changchun University of Science and Technology, Changchun 130022, China

(Received 20 June 2021; revised manuscript received 25 July 2021; accepted manuscript online 7 August 2021)

A theory of multiphoton photoemission is derived to explain the experimentally observed monotonic decrease with the wavelength in the electron yield of TiO₂ nanoparticles (NPs) by as large as four orders of magnitude. It is found that the fitting parameter corresponds to the energy position of Ti3d e_g and t_{2g} states, and the derived theory is a novel diagnostic of excited states in the conduction band, very importantly, applicable to individual NPs. The difference between four-photon slope NPs and three-photon slope NPs is attributed to the difference in defect density. The success of the theory in solving the puzzling result shows that thermal emission from high-lying levels may dominate over direct multiphoton ionization in solids when the photon number larger than four is required.

Keywords: multiphoton photoemission, nanoparticles, thermal emission, TiO₂

PACS: 42.50.Hz, 42.65.Sf, 42.79.Ek

DOI: 10.1088/1674-1056/ac1b8d

1. Introduction

Bulk gold (Au) is the highest chemically inert metal,^[1] but nano-sized Au nanoparticle (NP) is one of the most chemically active materials.^[2] Understanding how a chemically inert material changes to a highly active catalyst is a major topic in nanoscience.^[3–14] Previous papers assumed the Fermi level as the ground state of energetic electrons, called “hot electrons”,^[7,10–13] which means that the barrier height, ΔE , for electron transfer is the same in NPs and bulk. Then, there is no advantage of NPs over bulk materials in terms of electron transfer. We are proposing^[15,16] that high chemical activities of NPs originate in the generation of excited states in the conduction band, by which ΔE is lowered in NPs. TiO₂ is one of the most important materials as catalysts and its properties were studied by many people.^[17–22] The number of papers discussing dye-sensitized nanocrystalline TiO₂ as a low-cost high-efficiency solar cell increased exponentially since 1990.^[23–26] Presently, perovskite-type solar cells (PSC) are studied and most PSCs use TiO₂ as an electron transfer layer.^[27–32]

When studying electron transfer in NPs, observing individual NP is important as was emphasized by Beane *et al.*^[33] Photoemission electron microscopy (PEEM) having tens-nm spatial resolution^[34,35] is one of the best tools for studying electron transfer reactions in individual NPs. PEEM observes electrons ejected into the vacuum, and multiphoton photoemission (*m*-PPE) is a powerful technique for ejecting electrons

into the vacuum.^[36–42] We found an excited state in TiO₂ NPs at 0.78 eV above the conduction band minimum by using the two-color pump-probe technique using the fundamental and second harmonic of a femtosecond laser.^[15,16] The lifetime of the discovered excited state was longer than 4 ps, which is a few orders of magnitude longer than the lifetime reported for single crystals. This finding strongly supports our claim that the secret of nanomaterials is in the generation of excited states having a long lifetime.

While the excited state having a long lifetime was discovered, there remained a mystery in our previous work.^[15,16] The brightness of PEEM images monotonically decreased with the excitation wavelength by as large as four orders of magnitude. When the ionization energy or the electron affinity is E_g , electrons in the valence band or at the conduction band bottom are excited to vacuum by photons having photon energy $h\nu$ larger than $h\nu_0 = E_g/n$ when the excitation is an n -photon process. We can tell the number of photons from the slope of the dependence of particle brightness, B , on laser intensity, I , $B = a(h\nu)I^n$ in a log–log plot, where $a(h\nu)$ is called an excitation spectrum. When the photon energy $h\nu$ is smaller than $h\nu_0$, one more photon is required for the ionization. The brightness of the $(n+1)$ -photon process will be lower than the n -photon process, and the brightness should make a big jump at $h\nu_0$. However, no jump was observed and the excitation spectrum $a(h\nu)$ monotonically increased at higher photon energy. The present theory was derived to solve the puzzle.

*Project supported by the National Natural Science Foundation of China (Grant Nos. 91850109, 11474040, 61605017, and 61775021) and the “111” Project of China (Grant No. D17017).

[†]Corresponding author. E-mail: linjqin@cust.edu.cn

[‡]Corresponding author. E-mail: tomie@cust.edu.cn

For reproducing the observed excitation spectrum we need to assume two conditions: (i) the electrons in the excited states are instantly thermalized and (ii) the number of $(n + 1)$ -photon ionized electrons is smaller than the number of energetic electrons in the thermal distribution tail of the n -photon excited electrons.

The energy, $E(k)$, of electrons in excited states disperses with the wavenumber, k , of electron motion as

$$E(k) = E_{\text{exc}} + \left(\frac{h}{2\pi}\right)^2 \frac{k^2}{2m^*},$$

where m^* and h are an effective electron mass and the Planck constant. E_{exc} is the potential energy of the excited state and the second term is the kinetic energy of electrons. This dispersion was confirmed in angle-resolved electron emission measurements.^[43–49] At high power laser illumination for observing higher-order m -PPE, many electrons can coexist in excited states, and the energy distribution will follow the Boltzmann distribution by collisions among electrons. Thus, the first condition will be justified.

There are a large number of papers reporting two-photon m -PPE, 2PPE,^[36–42] but few report higher-order m -PPE with $m > 2$.^[41] Only two^[49,50] in our survey reported identical spectra for 2PPE and 3PPE, in which an intensity ratio of 3-PPE to 2PPE was about 10^{-4} . Hence, if the temperature, kT , of the electron gas in the excited state is high enough so that $\exp(-\Delta E/kT) > 10^{-4}$ where ΔE is the energy difference of the excited state from the vacuum level, the thermal emission from the excited state overwhelms the emission of directly photo-excited electrons by absorbing one more photon. In fact, we reported that thermal emission dominated over m -PPE in the case of Au NPs.^[51] As discussed in Ref. [51], non-integer m -PPE reported in many papers^[52–56] are explained by thermal emission. The present theory also explains why the number of reports of m -PPE with m larger than three is very few.^[41]

The derived theory serves as a novel diagnostic of the excited state in the conduction band. The observed NPs were classified into two groups; three-photon (3-photon NPs) and four-photon excited particles (4-photon NPs). The parameter for fitting to the data of 4-photon NPs confirmed the Ti3d e_g state close into the vacuum level located at 5.7 eV above the top of the valence band. The fitting parameter for 3-photon NPs confirmed a direct bandgap of 3.6 eV from O2p to Ti3d t_{2g} at the X point in the Brillouin zone. These states are different from the state revealed by the two-color pump-probe technique.^[15,16]

2. Theory of multiphoton photoemission

We consider n -photon excitation of valence band electrons to the excited state at E_G above the valence band top

as shown in Fig. 1. Electrons with binding energy E_B smaller than E_0 , where

$$E_0 = nh\nu - E_G, \quad (1)$$

are excited to the excited state. Here, $h\nu$ is the photon energy and the binding energy is measured from the valence band top.

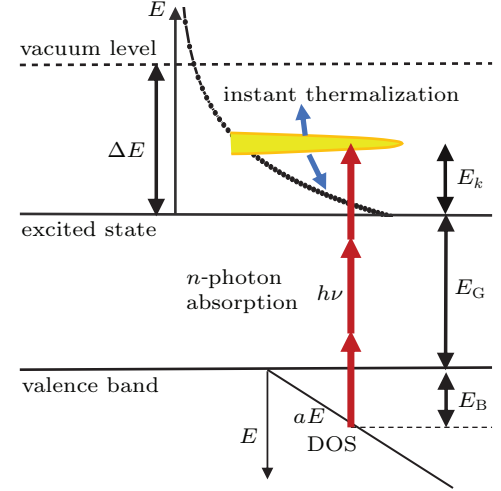


Fig. 1. N -photon excited electrons are instantly thermalized and electrons with kinetic energy exceeding ΔE at the tail of the Boltzmann distribution escape into the vacuum. Excess energy above the excited state, E_k , heats the electron gas.

Expressing the density of states of the valence band as $D(E)$, the number of electrons excited to the excited state, N_e , is given by

$$N_e = (\alpha N_{\text{ph}})^n \int_0^{E_0} D(E_B) dE_B, \quad (2)$$

where α is the one-photon absorption efficiency and N_{ph} is the number of photons irradiating the NP. For simplicity, α is assumed constant in all n -th excitation. The energy $E_B + E_G$ is consumed to excite electrons to the excited state, and the excess energy $E_k = nh\nu - (E_B + E_G)$ is stored in the electron gas as heat. The total heat energy E_{total} is calculated as

$$E_{\text{total}} = (\alpha N_{\text{ph}})^n \int_0^{E_0} E_k D(E_B) dE_B. \quad (3)$$

Assuming that the density of states $D(E)$ increases linearly with the binding energy,

$$D(E) = aE, \quad (4)$$

the N_e and E_{total} are then respectively calculated as

$$N_e = \left\{ \frac{a(\alpha N_{\text{ph}})^n}{2} \right\} E_0^2, \quad (5)$$

$$E_{\text{total}} = \left\{ \frac{a(\alpha N_{\text{ph}})^n}{6} \right\} E_0^3. \quad (6)$$

We assume that excited electrons are instantly thermalized and that the energy distribution is given by

$$g(E) = \left(\frac{N_e}{kT} \right) \exp\left(-\frac{E}{kT} \right). \quad (7)$$

The temperature is given by

$$E_{\text{total}} = N_e \left(\frac{3}{2} \right) kT. \quad (8)$$

From Eqs. (5), (6), and (8), the temperature T is obtained as

$$kT = \frac{2}{9} E_0. \quad (9)$$

Electrons with the kinetic energy larger than ΔE , defining the energy difference between the vacuum level and the ground state of the excited state, can escape into the vacuum. The number of escaped electrons N_{emit} is given by

$$N_{\text{emit}} = N_e \exp(-\Delta E/kT). \quad (10)$$

Substituting Eqs. (5) and (9) into Eq. (1), we get

$$N_{\text{emit}} = \left\{ \frac{a(\alpha N_{\text{ph}})^n}{2} \right\} E_0^2 \exp\left(-4.5 \frac{\Delta E}{E_0}\right). \quad (11)$$

When the density-of-states function differs from Eq. (4), equations (9) and (11) can be generalized in terms of a parameter p ,

$$kT = pE_0, \quad (12)$$

$$N_{\text{emit}} = \left\{ \frac{a(\alpha N_{\text{ph}})^n}{2} \right\} E_0^2 \exp\left(-\frac{\Delta E}{pE_0}\right). \quad (13)$$

Absorption of laser energy by electrons in the excited states can raise the temperature of the electron gas. Previously, we observed this phenomenon in Au NPs at a high laser power.^[51] However, the present theory ignores this additional heating for simplicity.

The above theory is valid under the following conditions.

(I) The electrons in the excited states are instantly thermalized. This condition requires the excitation of many electrons in one NP. (II) The electron gas is not further heated by the laser. (III) The electron energy distribution follows the Boltzmann distribution. (IV) The number of $(n+1)$ -photon-ionized electrons is smaller than the number of energetic electrons in the thermal distribution tail of the n -photon excited electrons.

From Eq. (9), we know the temperature is independent of the laser intensity, whereas, in usual thermionic emission as observed in our previous study,^[51] the emission intensity increases exponentially with the laser power which raises the temperature.

3. Experimental results

We illustrate how the theory reveals the excited states. Anatase TiO₂ NPs of nominal diameter 100 nm were sparsely dispersed on an n-type Si wafer as shown in Fig. 2(a). The NPs were illuminated by 150-fs-width laser pulses and the electrons ejected into the vacuum were imaged by PEEM which

has a nominal spatial resolution of 40 nm. The electron image was intensity-magnified by a microchannel plate (MCP), and the fluorescent image on the phosphor after the MCP was recorded by a charge-coupled device camera. The image brightness is proportional to the electron yield. The laser is tunable from 700 nm to 900 nm and operates at 76 MHz. The experimental method is detailed in our previous work.^[15]

Figure 2(b) plots the brightness *versus* laser power at three wavelengths: 700 nm (circles), 760 nm (triangles), and 780 nm (stars). Most of the NPs yielded a 4-photon absorption slope with the rest yielding a 3-photon absorption slope. As representatives of the four-photon and three-photon excited particles, we selected NPs A and B, respectively, enclosed in the amber circles in Fig. 2(a).

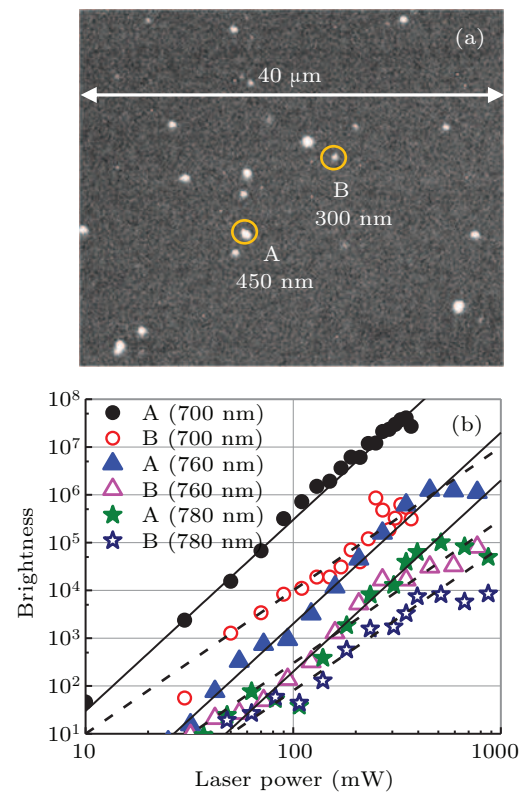


Fig. 2. (a) PEEM image of TiO₂ NPs dispersed on a Si wafer. Two TiO₂ NPs (A and B enclosed in amber circles) are selected as representative NPs. (b) Brightness *versus* laser power at three laser wavelengths. Filled and open symbols are the data of NP A and NP B, respectively. In most of the NPs (represented by NP A), the brightness increased with a 4-photon slope with the remaining NPs (represented by NP B) yielded a 3-photon slope.

The sizes of NP A and NP B were 3 pixels (450 nm) and 2 pixels (300 nm), respectively. Strictly speaking, both NPs are clusters of NPs, but here we call them NPs.

Figure 3 shows the wavelength dependence of the brightness at the 200-mW laser power for NPs A and B. The reference power of 200 mW for the excitation spectrum was chosen for the following two reasons. At power higher than 500 mW, the data points deviate from the linear slope in the log-log plot, and the reference power should be smaller than 500 mW. At lower power, NPs were darker and the accuracy of the brightness is poorer. So, higher reference power is better in terms of

the reliability of the data. The electron yield decreased monotonically from 700 nm (1.78 eV) to 790 nm (1.57 eV). This result was unexpected for two reasons. First, the ionization energy $E_I = \Delta E + E_G$ from the valence band top is about 7.5 eV in TiO_2 .^[57] Even for the oxygen-vacancy defect level lying at about 1 eV below the Fermi level,^[17–22] the ionization energy is about 5.5 eV, which is larger than the energy of 4.71 eV for three photons of 1.57-eV light. The second was that the brightness monotonically decreased by as large as four orders of magnitude from 700 nm to 790 nm in NP A (a 4-photon slope NP).

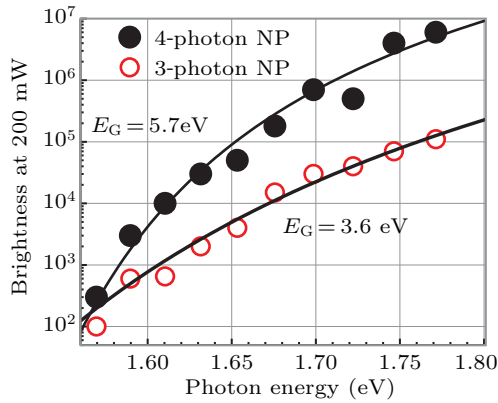


Fig. 3. Photon-energy dependence of the electron yield of the two TiO_2 NPs (A and B shown in Fig. 2(a)) under the 200-mW laser. The brightness increase (up to four orders of magnitude) is quite well reproduced by Eq. (11) (solid curves). The fitting parameter E_G was 5.7 eV for NP A and 3.6 eV for NP B.

Although some resonance transition is possible, the resonance transition should manifest as discrete peaks rather than a monotonic increase. Furthermore, the resonance enhancement will be only about one order of magnitude.

Two mysteries are solved by the derived theory. As shown by the solid curves in Fig. 3, equation (11) quite well reproduces the observed excitation spectra. Here we assumed $\Delta E + E_G = 7.5$ eV, the ionization energy given in Toyoda *et al.*^[57] The best fittings were obtained with E_G of 5.7 eV for NP A and 3.6 eV for NP B.

The three and four orders of magnitude differences in the brightness of NPs A and B at 700 nm (1.77 eV) and 790 nm (1.57 eV) were caused by the E_0 term ($= nh\nu - E_G$) in the exponential of Eq. (11). For example, when $n = 4$, $\Delta E = 1.8$ eV, and $E_G = 5.7$ eV, the value of $\exp(-4.5\Delta E/E_0)$ is 2.9×10^{-3} at 700 nm, and 8.1×10^{-7} at 790 nm. The factor E_0^2 in Eq. (11) further widens the brightness difference. When $nh\nu$ is close to E_G , $E_0 = nh\nu - E_G$ is small, the temperature kT of the electron gas is low, and the number of thermally excited electrons that can escape into the vacuum reduces drastically. Because electrons are thermally excited from the excited state, $nh\nu$ can be smaller than the ionization energy. Even at the shortest wavelength in our experiment (700 nm), the 4-photon energy of 7.08 eV was below the ionization energy of 7.5 eV. In addition, although NP B was dark, some electrons in the valence

band were ejected into the vacuum with a total photon energy of only 4.71 eV for three photons of 790-nm light. Therefore, thermionic emission has a great effect on photoemission. Thermionic emission has not been discussed in the past.^[52–56]

4. Discussion

First, we comment on the accuracy of the fitting parameter E_G . As discussed above, the rapid drop of brightness at smaller photon energy in Fig. 3 was caused by the decreased excess energy $E_0 = nh\nu - E_G$ in the exponential of Eq. (11). The choices of ΔE and the parameter p have only a small effect on the value of E_G . In fitting the data in Fig. 3, we assumed the ionization energy of $\Delta E + E_G = 7.5$ eV. When the ionization energy is decreased even to 5.5 eV, the fitting parameter E_G increases by only 0.1 eV.

The observed E_G can be interpreted by knowing the electronic structure of TiO_2 shown in Fig. 4(a). The bandgap energy between the valence band top and the conduction bottom of anatase TiO_2 is 3.2 eV.^[57,68] As the ionization energy,^[57,68] defined as the energy of the vacuum level from the valence band top, we assume 7.5 eV as reported by Toyoda *et al.*^[57]

The E_G of 3.6 eV obtained by fitting Eq. (11) to the NP B data in Fig. 3 disagrees with the established value of 3.2 eV. However, our $E_G = 3.6$ eV for NP B is considered to correspond to the direct bandgap. Figure 4(b) schematically shows the band structure calculated by Daude *et al.*^[69] According to their calculation, both the top of the valence band and the bottom of the conduction band are at the Γ point in the Brillouin zone, but the transition between these levels is forbidden. The bandgap energy of 3.2 eV observed by many groups is the energy of the “indirect transition” between the Γ and X points. The allowed “direct transition” is at the X point. Reported direct bandgap energies range from 3.5 eV to 3.8 eV.^[57,61,64,65,70] Our value agrees with the value calculated by Daude *et al.*^[69]

Next, we discuss the $E_G = 5.7$ eV obtained by fitting Eq. (11) to NP A. Vos^[71] reported that the conduction band of TiO_2 comprises two groups; the lower group is the triple-degenerated $2t_{2g}$ state and the upper group is the doubly degenerated $3e_g$ state as shown in Fig. 4(a). The energy separation of the t_{2g} and e_g states was measured as 2.1 eV by Fisher^[72] estimated from the x-ray absorption spectrum. Our observed state at $E_G = 5.7$ eV above the valence band top is considered to correspond to the transition from O2p to the Ti3d e_g state.

In fact, an excited state close to $E_G = 5.7$ eV was observed by Argondizzo *et al.*^[73] They observed several times enhancement of the photoemission for a 3.66 eV laser than at 3.22 eV and 3.95 eV. They irradiated a single crystal of rutile TiO_2 (111) with 20-fs laser pulses. They explained that the

defect states lying 0.85 eV below the Fermi level were two-photon ionized. They also explained that the 3.66-eV light was in resonance with the transition from the defect states to the e_g state as indicated by the thick red arrow in Fig. 4(a). The bandgap energy of rutile TiO_2 is 3.0 V. Therefore, assuming that the Fermi level is very close to the conduction band bottom, the energy of the e_g state from the valence band top is 5.81 eV ($= 3 + 3.66 - 0.85$) in their experiment for the crystal, and close to our observed value for NPs. Daude *et al.*^[69] reported the detailed band structure of TiO_2 . According to their calculation as schematically shown in Fig. 4(b), the direct transition between the Ti 3d $3e_g$ and O 2p $1t_g$ states takes place at the X point with the transition energy of 5.7 eV. This value agrees with our fitting parameter of $E_G = 5.7$ eV for the NP A data in Fig. 3.

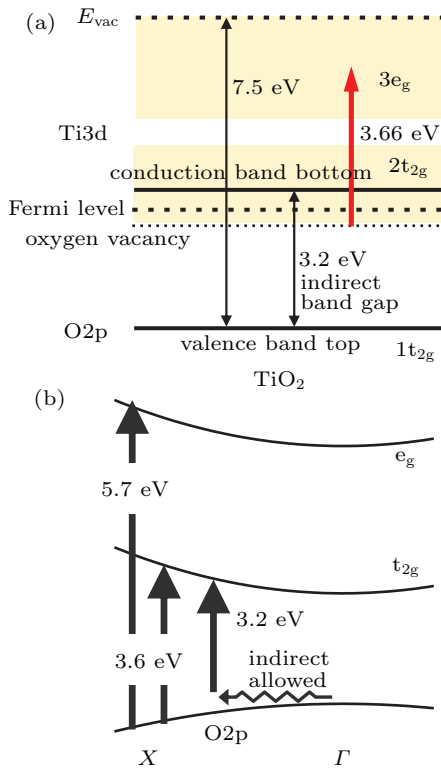


Fig. 4. (a) Electronic structure of TiO_2 obtained from references. The thick red arrow shows the transition to the e_g level, which assists 2-photon ionization of the defect level lying below the Fermi level reported by Argondizzo *et al.*^[73] (b) Schematic diagram of the band structure calculated by Daude *et al.*^[69]

Thus, we confirmed that the value of E_G estimated by our theory is quite accurate. Readers should note that these values were estimated not from a single crystal but a single cluster of NPs.

We could attribute the difference between the 4-photon and 3-photon NPs to the difference in their defect densities. Thermionic electron emission is far easier from the high-lying e_g state than from the low-lying t_{2g} state. We put concrete numbers. When $h\nu = 1.77$ eV, E_0 in Eq. (11) is 1.38 eV for 4-photon excitation to the $E_G = 5.7$ eV state and 1.71 eV for 3-photon excitation to the $E_G = 3.6$ eV state. When the

ionization energy is 7.5 eV, ΔE is 1.8 eV and 3.9 eV for the $E_G = 5.7$ eV state and the $E_G = 3.6$ eV state, respectively. Then, $\exp(-4.5\Delta E/E_0)$ is 2.8×10^{-3} for the $E_G = 5.7$ eV state and 3.5×10^{-5} for the $E_G = 3.6$ eV state. However, four-photon excitation occurs with a very low probability than that of three-photon excitation. Bisio *et al.*^[49] and Banfi *et al.*^[50] observed a replica of energy spectra for two-photon and three-photon excitations of Cu(001) and Ag(100), respectively, which is the evidence of above-threshold photoemission. The intensity of the 3-photon excited Fermi edge was four orders of magnitude weaker than that of the 2-photon excited Fermi level. Therefore, thermionic emission from the low-lying t_{2g} state, which requires only 3 photons, is more probable than from the high-lying e_g state. However, if there is a high density of defects, they assist the four-photon excitation to the e_g state as shown in Fig. 5. Hence, we can interpret that 4-photon NPs have a high density of defects. In the case of Argondizzo *et al.*,^[73] the e_g state assisted the ionization of the defect states, but in our case, the defects assisted the excitation of valence electrons to the e_g state.

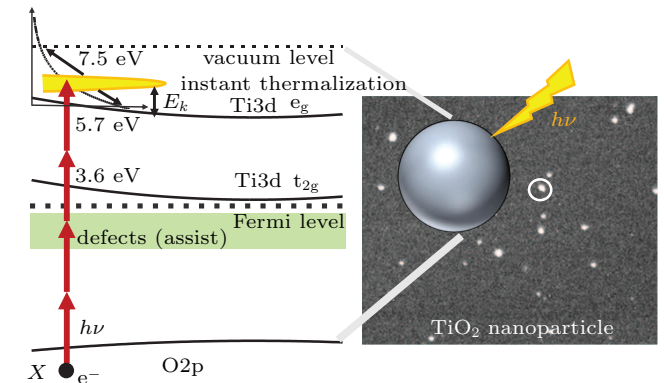


Fig. 5. Multiphoton excited electrons are instantly thermalized. The excess energy E_k above the excited state heats the electron gas, and electrons with kinetic energies above ΔE at the tail of the Boltzmann distribution escape into the vacuum, providing the PEEM image. When applied to the photon energy dependence of the electron yield, the theory reveals the excited states. Four-photon excitation to the e_g state is assisted by the defect states lying below the Fermi level.

Figure 5 summarizes what our theory revealed. The Ti3d e_g state at 5.7 eV above the valence band top is 4-photon excited from O2p. The excited electrons are instantly thermalized and the electrons at the tail of the Boltzmann distribution escape into the vacuum. The excess energy E_k heats the electron gas in the excited state. With increasing the photon energy, the excess energy increases, leading to a drastic increase in the electron yield. Four-photon excitation of the e_g state can be assisted by the defect state below the Fermi level. Allowed direct transition from the O2p to the t_{2g} level at the X point was also revealed by fitting the theory to the data of 3-photon slope NPs.

We now discuss the thermalization of electrons in the excited state. According to previous works, electrons are thermalized in about 10 fs^[74,75] far shorter than the pulse width

of 150 fs in the present experiment. Furthermore, in previous papers reporting the energy spectra, all spectra were thermalized,^[11,55,75,78] supporting our instant thermalization assumption. Instant thermalization requires strong electron-electron collisions and excitation of many electrons in one NP. Accordingly, the present diagnostic requires high-intensity femtosecond irradiation.

In the Introduction of Ref. [51], we mentioned that there was a puzzle of non-integer power law in *m*-PPE.^[52–56] Gloskovskii *et al.*^[55] reported that slopes, *n*, in a log–log plot of the brightness of PEEM images on laser intensity were *n* = 2.98, 3.2, and 3.7, respectively in different areas of different particle sizes for a stripe of Ag film consisting of different particle sizes from a few to a few tens nm. Schmidt *et al.*^[53] observed *n* = 3.5 for metallic adsorbates on Si(111), Fecher *et al.*^[54] reported a mapping of slopes between *n* = 2 and *n* = 3 for hot spots for pentacene on silicon, and Georgiev *et al.*^[56] observed non-integer slopes of *n* = 2.3 ± 0.3 for hot spots on a well-prepared Cu(001). Aeschlimann *et al.*^[52] reported *n* = 2.8 at electron kinetic energy of 0.8 eV and *n* = 3.2 at 2.5 eV. The success of the derived theory solving our mystery dissolves the puzzle in the past. When the electrons in the excited states are instantly thermalized and electrons are emitted thermally, the slope is not simply determined by the number of photons to reach the excited states. In the derived theory, additional laser heating of electrons in the excited states was ignored for simplicity, but in many cases, additional heating can be very large as we observed for Au NPs.^[51] Then, the slope of electron emission can largely deviate from an integer value and the deviation will depend on the property of the excited states. In the derived theory, the electron temperature given by Eq. (12) is determined by $E_0 = nh\nu - E_G$ which is independent of laser power. The factor depending on laser power is $\{(a(\alpha N_{ph})^{n+1})/2\}$ which follows an integer power scale. When additional laser heating is not negligible, the electron temperature is given by $kT = pE_0 + hI$, where hI is the contribution of additional laser heating. Then, $N_{emit} = N_e \exp(-\Delta E/kT)$ increases with a non-integer slope. The slope changes with power and can be as large as 10 as was observed in our experiment for Au NPs.^[51]

The derived theory also explains the difficulty of observing higher-order *m*-PPE whose reasons were discussed in Winkelmann *et al.*^[41] To observe higher-order *m*-PPE, higher irradiation is required because the electron yield decreases by about 10^{-4} for every higher order. Then the temperature of the electron gas can be very high and thermal emission even from low lying states can be very large. This argument is valid when electrons are instantly thermalized, which can be realized in solids. In gases, molecular density is low, electrons in the excited states may not be thermalized, and higher-order multiphoton ionization can be detected.

Finally, we discuss the expected structure of excitation spectrum of *m*-PPE over the whole photon energy. At the very high photon energy region, $\Delta E < E_0 = nh\nu - E_G$, the factor $\exp(-4.5\Delta E/E_0)$ in Eq. (11) saturates to 1, and the NP brightness saturates for *n*-photon excitation. Then, at certain photon energy, (*n* − 1)-photon excitation dominates over *n*-photon excitation. For example, in the case of NP A, $E_G = 5.7$ eV as seen in Fig. 3, and $\Delta E = 1.8$ eV. Then, at $h\nu = 2.1, 2.2$, and 2.3 eV, the factor $\exp(-4.5\Delta E/E_0)$ are 0.05, 0.07, and 0.1 for *n* = 4 and 1.37×10^{-6} , 1.23×10^{-4} , and 0.0012 for *n* = 3, respectively. The brightness for *n* = 3 increases steeply with the photon energy while it is saturating for *n* = 4. When the excitation efficiency is four orders of magnitude larger for *n* = 3 than for *n* = 4, 3-PPE is brighter than 4-PPE at $h\nu > 2.2$ eV. Similarly, 2-PPE dominates over 3-PPE above 3.3 eV. The steep rise and saturation of the brightness seen in Fig. 3 will be repeated with decreasing *n* for the whole photon energy.

5. Summary

In summary, a theory of multiphoton photoemission was derived and the excited states in the conduction band of a single TiO₂ NP were revealed by applying the theory. In the theory, photo-excited hot electrons are instantly thermalized, the excess energy of exciting valence band electrons to the excited state heats the electrons in the excited state, and hot electrons in the high energy tail of the thermal distribution escape into the vacuum.

The theory was applied to the experimentally observed photon–energy dependence of the electron yield of TiO₂ NPs. In most of the NPs, the yield increased with a 4-photon slope with the remainder exhibiting a 3-photon slope. The electron yields at 700 nm and 790 nm differed by as large as four orders of magnitude in the 4-photon slope NPs, and by three orders of magnitude in the 3-photon slope NPs. The derived theory well reproduced the observed excitation spectrum. From the fitting parameters, the excitation energies of the excited states were estimated as 5.7 eV and 3.6 eV in 4-photon and 3-photon excited NPs, respectively. The excited states were respectively assigned as the e_g and t_{2g} states. The estimated values agreed with those of previous observations and with the values calculated by Daude *et al.*^[69] Four photon excitation of valence band electrons to the e_g state is presumably assisted by the defect level below the Fermi level.

The success of reproducing the wavelength dependence of electron yield as large as four orders of magnitude proved that electrons in the excited states can be instantly thermalized leading to strong thermal emission from the levels below the vacuum level. This mechanism explains the non-integer slope of *m*-PPE and the difficulty of observing higher order *m*-PPE.

References

- [1] Schwank J 1983 *Gold Bull.* **18** 103
- [2] Haruta M, Kobayashi T, Sano H and Yamada N 1987 *Chem. Lett.* **16** 405
- [3] Janssens T V W, Clausen B S, Hvolbæk B, Falsig H, Christensen C H, Bligaard T and Nørskov J K 2007 *Topics in Catalysis* **44** 15
- [4] Overbury S H, Schwartz V, Mullins D R, Yan W and Dai S 2006 *J. Catalysis* **241** 56
- [5] Fujita T, Guan P, McKenna K, Lang X, Hirata A, Zhang L, Tokunaga T, Arai S, Yamamoto Y, Tanaka N, Ishikawa Y, Asao N, Yamamoto Y, Erlebacher J and Chen M 2012 *Nat. Mater.* **11** 775
- [6] Linic S, Christopher P and Ingram D B 2011 *Nat. Mater.* **10** 911
- [7] Mukherjee S, Libisch F, Large N, Neumann O, Brown L V, Cheng J, Lassiter J B, Carter E A, Nordlander P and Halas N J 2013 *Nano Lett.* **13** 240
- [8] Clavero C 2014 *Nat. Photon.* **8** 95
- [9] Chalabi H, Schoen D and Brongersma M L 2014 *Nano Lett.* **14** 1374
- [10] Kumar D, Lee A, Lee T, Lim M and Lim D K 2016 *Nano Lett.* **16** 1760
- [11] Tan S, Argondizzo A, Ren J, Liu L, Zhao J and Petek H 2017 *Nat. Photon.* **11** 806
- [12] Kazuma E, Jung J, Ueba H, Trenary M and Kim Y 2018 *Science* **360** 521
- [13] Zhang Y, He S, Guo W, Hu Y, Huang Ji, Mulcahy J R and Wei W D 2018 *Chem. Rev.* **118** 2927
- [14] Zu S, Han T, Jiang M, Liu Z, Jiang Q, Lin F, Zhu X and Fang Z 2019 *Nano Lett.* **19** 775
- [15] Li B, Li H, Yang C, Ji B, Lin J and Tomie T 2019 *AIP Adv.* **9** 085321
- [16] Li B, Li H, Yang C, Ji B, Lin J and Tomie T 2020 *Catalysts* **10** 916
- [17] Cronmeyer D C 1952 *Phys. Rev.* **87** 876
- [18] Breckenridge R G and Hosler W R 1953 *Phys. Rev.* **91** 793
- [19] Ghosh A M, Wakim F G and Addiss R R Jr. 1969 *Phys. Rev.* **184** 979
- [20] Wendt S, Sprunger P T, Lira E, Madsen G K H, Li Z, Hansen J Ø, Matthiesen J, Blekinge-Rasmussen A, Lægsgaard E, Hammer B and Besenbacher F 2008 *Science* **320** 1755
- [21] Henderson M A 2011 *Surf. Sci. Rep.* **66** 185
- [22] Zhang Z and Yates Jr J T 2012 *Chem. Rev.* **112** 5520
- [23] Fujishima A and Honda K 1972 *Nature* **238** 37
- [24] O'Regan B and Grätzel M 1991 *Nature* **353** 737
- [25] Fujishima A, Zhang X and Tryk D K 2008 *Surf. Sci. Rep.* **63** 515
- [26] Furube A and Hashimoto S 2017 *NPG Asia Mater.* **9** e454
- [27] Kojima A, Teshima K, Shirai Y and Miyasaka T 2009 *J. Am. Chem. Soc.* **131** 6050
- [28] Lee M M, Teuscher J, Miyasaka T, Murakami T N and Snaith H J 2012 *Science* **338** 643
- [29] Seo J, Noh J H and Seok I 2016 *Acc. Chem. Res.* **49** 562
- [30] Giordano F, Abate A, Correa Baena J P, Saliba M, Matsui T, Im S H, Zakeeruddin S M, Nazeeruddin M K, Hagfeldt A and Grätzel M 2016 *Nat. Commun.* **7** 1
- [31] Ruankham P and Sagawa T 2018 *J. Mater. Sci.: Mater. Electron.* **29** 9058
- [32] Kaewprajak A, Kumnorkaew P and Sagawa T 2019 *J. Mater. Sci.: Mater. Electron.* **30** 4041
- [33] Beane G, Devkota T, Brown B S and Hartland G V 2019 *Rep. Prog. Phys.* **82** 016401
- [34] Dąbrowski M, Dai Y and Petek H 2020 *Chem. Rev.* **120** 6247
- [35] Bauer E 2012 *J. Electron. Spectr. Rel. Phenom.* **185** 314
- [36] Bokor J 1989 *Science* **246** 1130
- [37] Schmittenmaer C A, Aeschlimann M, Elsayed-Ali H E, Miller R J D, Mantell D A, Cao J and Gao Y 1994 *Phys. Rev. B* **50** 8957
- [38] Haight R 1995 *Surf. Sci. Rep.* **21** 275
- [39] Petek H and Ogawa S 1997 *Prog. Surf. Sci.* **56** 239
- [40] Weinelt M 2002 *J. Phys.: Condens. Matter* **14** R1099
- [41] Winkelmann A, Chiang C T, Bisio F, Lin W C, Kirschner J and Petek H 2010 *Dynamics at Solid State Surfaces and Interfaces: Vol. 1: Current Developments* (Germany: WILEY-VCH) pp. 33–49
- [42] Bauer M, Marienfeld A and Aeschlimann M 2015 *Prog. Surf. Sci.* **90** 319
- [43] Woodruff D P, Smith N V, Johnson P D and Royer W A 1982 *Phys. Rev. B* **26** 2943
- [44] Johnson P D and Smith N V 1983 *Phys. Rev. B* **27** 2525
- [45] Kevan S 1983 *Phys. Rev. B* **28** 4822
- [46] Giesen K, Hage F, Riess H J, Steinmann, Haight W R, Beigang R, Dreyfus R, Avouris Ph and Himpel F J 1987 *Physica Scripta* **35** 578
- [47] Kubiak G D 1988 *Surf. Sci.* **201** L475
- [48] Strocov V N, Claessen R, Nicolay G, Hüfner S, Kimura A, Harasawa A, Shin S, Kakizaki A, Starnberg H I, Nilsson P O and Blaha P 2001 *Phys. Rev. B* **63** 205108
- [49] Bisio F, Nyólt M, Franta I J, Petek H and Kirschner J 2006 *Phys. Rev. Lett.* **96** 087601
- [50] Banfi F, Giannetti C, Ferrini G, Galimberti G, Pagliara S, Fausti D and Parmigiani F 2005 *Phys. Rev. Lett.* **94** 037601
- [51] Li B, Yang C, Li H, Ji B, Lin J and Tomie T 2019 *AIP Adv.* **9** 025112
- [52] Aeschlimann M, Schmittenmaer C A, Elsayed-Ali H E, Miller R J D, Cao J, Gao Y and Mantell D A 1995 *J. Chem. Phys.* **102** 8606
- [53] Schmidt O, Fecher G H, Hwu Y and Schoenhense G 2001 *Surf. Sci.* **687** 482
- [54] Fecher G H, Schmidt O, Hwu Y and Schoenhense G 2002 *J. Electron Spectr. Relat. Phenom.* **126** 77
- [55] Gloskovskii A, Valdaitsev D, Nepijko S A, Schoenhense G and Rethfeld B 2007 *Surf. Sci.* **601** 4706
- [56] Georgiev N, Martinotti D and Ernst H-J 2007 *Phys. Rev. B* **75** 085430
- [57] Toyoda T, Yindeesuk W, Okuno T, Akimoto M, Kamiyama K, Hayase S and Shen Q 2015 *RSC Adv.* **5** 49623
- [58] Anpo M, Shima T, Kodama S and Kubokawa Y 1987 *J. Phys. Chem.* **91** 4305
- [59] Tang H, Prasad K, Sanjinès R, Schmid P E and Lévy F 1994 *J. Appl. Phys.* **75** 2042
- [60] Serpone N, Lawless D and Khairutdinov R 1995 *J. Phys. Chem.* **99** 16646
- [61] Aoki A and Nogami G 1996 *J. Electrochem. Soc.* **143** L191
- [62] Boschloo G K, Goossens A and Schoonman J 1997 *J. Electrochem. Soc.* **144** 1311
- [63] Takikawa H, Matsui T, Sakakibara T, Bendavid A and Martin P J 1999 *Thin Solid Films* **348** 145
- [64] Wang Z, Helmersson U and Käll P O 2002 *Thin Solid Films* **405** 50
- [65] Hasan M M, Haseeb A, Saidur R, Msjuki H H and Hamdi M 2010 *Opt. Mater.* **32** 690
- [66] López R and Gómez R 2012 *J. Sol-Gel Sci. Technol.* **61** 1
- [67] Xu H, Reunchan P, Ouyang S, Tong H, Umezawa N, Kako T and Ye J 2013 *Chem. Mater.* **25** 405
- [68] Fujisawa J, Eda T and Hanaya M 2017 *Chem. Phys. Lett.* **685** 23
- [69] Daude N, Gout C and Jouanin C 1977 *Phys. Rev. B* **15** 3229
- [70] Liu B, Wen L and Zhao X 2007 *Mat. Chem. Phys.* **106** 350
- [71] Vos K 1977 *J. Phys. C: Solid State Phys.* **10** 3917
- [72] Fisher D W 1972 *Phys. Rev. B* **5** 4219
- [73] Argondizzo A, Cui X, Wang C, Sun H, Shang H, Zhao J and Petek H 2015 *Phys. Rev. B* **91** 155429
- [74] Link S and El-Sayed M A 1999 *J. Phys. Chem. B* **103** 8410
- [75] Bauer M and Aeschlimann M 2002 *J. Electron Spectr. Rel. Phenom.* **124** 225
- [76] Aeschlimann M, Schmittenmaer C A, Elsayed-Ali H E and Miller R J D 1995 *J. Chem. Phys.* **102** 8606
- [77] Knoesel E, Hotzel A, Hertel T, Wolf M and Ertl G 1996 *Surf. Sci.* **368** 76
- [78] Tan S, Argondizzo A, Wang C, Cui X and Petek H 2017 *Phys. Rev. X* **7** 011004